20. A. Zerr, G. Serghiou, R. Boehler, *Proceedings of the Fifth NIRIM International Symposium on Advanced Materials*, Tsukuba, Japan, 1 to 5 March 1998 (National Institute for Research in Inorganic Materials, Tsukuba, Japan, 1998), pp. 5–8.
21. E. Takahashi, *J. Geophys. Res.* **91**, 9367 (1986).
22. J. M. Brown and T. S. Shankland, *Geophys. J. R. Astron. Soc.* **66**, 579 (1981).
23. R. Boehler, *Annu. Rev. Earth Planet. Sci.* **24**, 15 (1996).
24. R. Boehler, *Philos. Trans. R. Soc. London Ser. A* **354**, 1265 (1996).
25. We thank V. Hillgren, B. Schulz-Dobrick, and G. Serghiou for helpful discussions and V. Hillgren, G. Serghiou, and the reviewers for constructive comments on the manuscript.

2 March 1998; accepted 18 May 1998

# A Reduction-Pyrolysis-Catalysis Synthesis of Diamond

**Yadong Li,* Yitai Qian,* Hongwei Liao, Yi Ding, Li Yang, Cunyi Xu, Fangqing Li, Guien Zhou**

**Diamond powder was synthesized through a metallic reduction-pyrolysis-catalysis route with the reaction of carbon tetrachloride and sodium at 700°C, in which the sodium was used as reductant and flux. This temperature is much lower than that of traditional methods. The x-ray powder diffraction patterns showed three strong peaks of diamond. The Raman spectrum showed a sharp peak at 1332 inverse centimeters, which is characteristic of diamond. Although the yield was only 2 percent, this method is a simple means of forming diamond.**

The properties of diamond materials, such as optical properties, high hardness, high thermal conductivity (*1*), and semiconductivity induced by doping, have led to considerable efforts to create diamond since the first report of diamonds synthesized through a high-pressure high-temperature process (*2*). Diamonds made with the TNT detonation method were composed of nanometer-sized spherical particles (*3, 4*). Micrometer-sized diamonds have been grown in a hydrothermal process using carbon, water, and metal near 800°C and at 1.4 kbar pressure, but diamond seeds were needed (*5, 6*). Chemical vapor deposition (CVD) (*7–10*) is a low-pressure synthetic route to the synthesis of polycrystalline diamond films, which uses $CH_4$ or $C_2H_2$ as a carbon source. Through the action of thermal filament–assisted CVD, plasma CVD, or combustion flame CVD, the carbon source decomposed to form active carbon (in the $sp^3$ hybrid state), which formed diamondlike structure films. In traditional organic synthesis, the Wurtz reaction (*11*) $R^1X + R^2X + 2Na \rightarrow R^1\text{–}R^2 + 2NaX$ can be used to form carbon-carbon bonds between alkyl groups. If $CCl_4$ is treated with Na under appropriate temperature and pressure, the carbon atoms could connect to form a three-dimensional network; such a network based on the $sp^3$ hybrid state could be diamond. Here, we selected $CCl_4$ as a carbon source to synthesize diamond by using Na as reductant and flux at 700°C in the presence of a metal catalyst (*2, 12*). Diamond was formed, although at a low yield (~2%). The process could be proposed as

$$CCl_4 + 4Na \xrightarrow[\text{Ni–Co}]{700°C} C(\text{diamond}) + 4NaCl \quad (1)$$

We call it the reduction-pyrolysis-catalysis (RPC) route. According to the free energy calculations $\Delta G°$ (diamond) = −416.7 kcal $mol^{-1}$ and $\Delta G°$ (graphite) = −417.4 kcal $mol^{-1}$, $CCl_4 + 4Na \rightarrow C(\text{diamond}) + 4NaCl$ and $CCl_4 + 4Na \rightarrow C(\text{graphite}) + 4NaCl$ are thermodynamically spontaneous. Formation of graphite (amorphous carbon) and diamond is possible, and the yield of graphite (amorphous carbon) and diamond may be determined by kinetics. X-ray powder diffraction (XRD) patterns showed three strong peaks of diamond [(111), (220), and (311)] and gave a lattice constant of 3.569 Å, which is near the reported value (*13*). The Raman spectrum showed a sharp peak at 1332 $cm^{-1}$, which represented diamond (*14*).

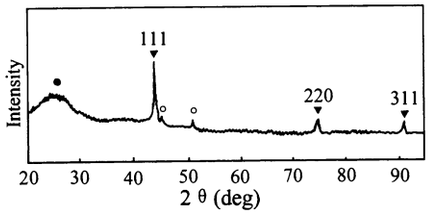


**Fig. 1.** X-ray diffraction pattern of sample. Diamond peaks, ▼; amorphous carbon, ●; Ni-Co alloy peaks, ○.

An appropriate amount of $CCl_4$ (5 ml) and an excess of metal Na (20 g) were put into a stainless steel autoclave of 50-ml capacity, and then several pieces of Ni-Co alloy (Ni:Mn:Co, 70:25:5 by weight) were added to the autoclave as a catalyst. The autoclave was maintained at 700°C for 48 hours and then allowed to cool to room temperature. At the beginning of the reduction, there was high pressure in the autoclave. However, as $CCl_4$ was reduced by metal Na, the pressure in the autoclave decreased. The products were washed with absolute ethanol, then with 6 mol $liter^{-1}$ HCl, and then with distilled water. The final powder was dried in an oven. A grayish-black powder was obtained with a density of 3.21 g $cm^{-3}$. This value is less than face-centered cubic diamond (3.51 g $cm^{-3}$) and may be due to the presence of a coating of amorphous carbon on the diamond.

The XRD pattern was recorded on a Rigaku D/max rA x-ray diffractometer with Cu Kα radiation [wavelength (λ) = 1.54178 Å]. The XRD patterns (Fig. 1) show three strong peaks of diamond [(111), (220), and (311)] and these patterns can be indexed to the cubic cell of diamond with a lattice constant $a$ = 3.569 Å, which is near the reported values (*13*). However, in the pattern, there is a stronger wide peak at ~26° (2θ), indicating a significant amount of amorphous carbon; and there are also weaker peaks, indicating the existence of a catalyst alloy after the product was washed with acid. These weaker peaks may appear because the alloy particles were coated by carbon and were

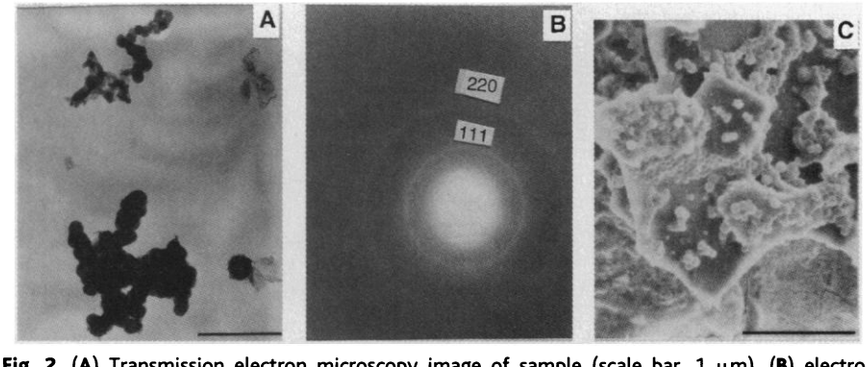


**Fig. 2.** (**A**) Transmission electron microscopy image of sample (scale bar, 1 μm), (**B**) electron diffraction pattern, and (**C**) SEM image (scale bar, 60 μm).

Structure Research Laboratory and Department of Chemistry, University of Science and Technology of China, Hefei, Anhui 230026, People's Republic of China.

*To whom correspondence should be addressed.

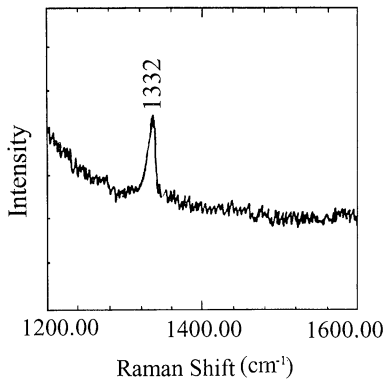


**Fig. 3.** Raman spectrum of sample.

resistant to acid solution. The existence of a small amount of catalyst alloy may increase the density value of the sample, whereas the amorphous carbon decreases this value. The x-ray result was consistent with the density value.

Transmission electron microscopy images and electron diffraction patterns were taken with a Hitachi H-800 transmission electron microscope. The micrograph (Fig. 2A) shows that the diamond aggregate consists of spherelike particles. Electron diffraction patterns (Fig. 2B) show two rings [(111) and (220)] of diamond and confirm the XRD result. Fig. 2C is a scanning electron microscope (SEM) image of the sample on a Ni-Co alloy plate (taken with a Hitachi X-650 SEM); this image shows that small particles are aggregated on the diamonds.

The Raman spectrum was produced at room temperature with a Spex 1403 Raman spectrometer. The Raman spectrum of the products (Fig. 3) exhibits an intense, sharp peak at 1332 $cm^{-1}$, indicating well-crystallized diamond.

Improvements in the process of synthesizing diamond are still needed. Much work is required to understand and control the reaction kinetics. Finding a better catalyst is very critical for the formation and growth of diamond crystal. Transitional metals (for example, Ni, Co, Mn, Fe, and Pt), their alloys, and their carbides may be the favorable catalysts (*2, 6*). In addition, substituting another halohydrocarbon carbon source (in the $sp^3$ hybrid state), such as $C_2Cl_6$, $CCl_4$, $CBr_4$, or a mixture of these, for $CCl_4$ may improve the process. It is reasonable to suppose that the addition of diamond seeds may increase the yield of diamond in the previously reported hydrothermal growth process (*6*). This method may provide a new means of producing diamond and other carbides, such as SiC, TiC, WC, and so forth.

**References and Notes**

1. J. E. Graebner, S. Jin, G. W. Kammlott, J. A. Herb, C. F. Gardinier, *Nature* **359**, 401 (1992).
2. F. P. Bundy, H. T. Hall, H. M. Strong, R. H. Wentorf, *ibid.* **176**, 51 (1955).
3. N. R. Gneiner, D. S. Phillips, J. D. Johnson, F. Volk, *ibid.* **333**, 440 (1988).
4. M. V. Thiel and F. H. Ree, *J. Appl. Phys.* **62**, 1761 (1987).
5. R. Roy, D. Ravichandran, P. Ravichandran, A. Bazian, *J. Mater. Res.* **11**, 1164 (1996).
6. X.-Z. Zhao, R. Roy, K. A. Cherian, A. Badzian, *Nature* **385**, 513 (1997).
7. W. G. Everssle, U.S. Patent 3,030,187 (1958); U. S. Patent 3,030,188 (1958); J. C. Angus, H. A. Wiu, W. S. Stanko, *J. Appl. Phys.* **39**, 2915 (1968); B. V. Spitsyn, L. L. Bouilov, B. V. Deryagin, *J. Cryst. Growth* **53**, 219 (1981); S. Mastumoto, Y. Sato, M. Kamo, N. Setaka, *Jpn. J. Appl. Phys.* **21**, L183 (1982); S. J. Harris, *Appl. Phys. Lett.* **56**, 2298 (1990).
8. A. Aisenberg and K. Chabot, *J. Appl. Phys.* **42**, 2953 (1971); E. G. Spencer, P. H. Schmidt, D. J. Joy, F. J. Sanssalone, *Appl. Phys. Lett.* **29**, 118 (1976); C. Weissmantal *et al.*, *Thin Solid Films* **72**, 19 (1980).
9. S. S. Lee, D. W. Minsek, D. J. Vestyck, P. Chen, *Science* **263**, 1596 (1994); D. S. Whitmel and R. Williamson, *Thin Solid Films* **35**, 255 (1976); L. Holland and S. M. Ojha, *ibid.* **48**, L17 (1976); M. Sokolowski, A. Sokolowska, B. Gokieli, A. Rusek, Z. Romanowski, *J. Cryst. Growth* **47**, 421 (1979); H. Vora and T. J. Moravec, *J. Appl. Phys.* **52**, 6151 (1981); K. Suzudi *et al.*, *Appl. Phys. Lett.* **50**, 728 (1987); Y. Muranaka, H. Yamashita, K. Sato, H. Miyadera, *J. Appl. Phys.* **67**, 6247 (1990); J. Lee, R. W. Collins, R. Messier, *Appl. Phys. Lett.* **70**, 1527 (1997).
10. J.-J. Wu and F. C.-N. Hong, *Appl. Phys. Lett.* **70**, 185 (1997).
11. I. L. Finar, *Organic Chemistry* (Longman, White Plains, NY, 1973), vol. 1, chap. 3, p. 76.
12. V. P. Novikov and V. P. Dymont, *Appl. Phys. Lett.* **70**, 200 (1997).
13. See supplementary x-ray data [Joint Committee on Powder Diffraction Standards (JCPDS) 6-0675].
14. S. A. Solin and A. K. Ramdas, *Phys. Rev. B* **1**, 1678 (1970).
15. We thank Y. C. Liu, H. Y. Fan, Y. H. Zhang, Q. X. Guo, and S. Q. Yu for helpful discussions. This work was supported by the National Natural Science Foundation of China and the National Nanometer Materials Climbing Project.

2 December 1997; accepted 3 June 1998

# MR Imaging Contrast Enhancement Based on Intermolecular Zero Quantum Coherences

**Warren S. Warren,* Sangdoo Ahn, Marlene Mescher, Michael Garwood, Kamil Ugurbil, Wolfgang Richter, Rahim R. Rizi, Jeff Hopkins, John S. Leigh**

A new method for magnetic resonance imaging (MRI) based on the detection of relatively strong signal from intermolecular zero-quantum coherences (iZQCs) is reported. Such a signal would not be observable in the conventional framework of magnetic resonance; it originates in long-range dipolar couplings (10 micrometers to 1 millimeter) that are traditionally ignored. Unlike conventional MRI, where image contrast is based on variations in spin density and relaxation times (often with injected contrast agents), contrast with iZQC images comes from variations in the susceptibility over a distance dictated by gradient strength. Phantom and in vivo (rat brain) data confirm that iZQC images give contrast enhancement. This contrast might be useful in the detection of small tumors, in that susceptibility correlates with oxygen concentration and in functional MRI.

Contrast in MRI is largely based on variations in spin density or relaxation times, sometimes enhanced by injected contrast agents such as gadolinium compounds. The relation between these parameters and tissue morphology is not always unique. Thus, it is not surprising that in some applications no combination of these parameters gives sufficient useful contrast. Even with brain imaging, particularly in the rapidly expanding field of functional MRI (*1*), contrast is frequently the limiting factor. New methods for contrast enhancement could thus improve soft tissue characterization, particularly if they correlate with physiologically important characteristics.

Here, we demonstrate a type of MRI based on detection of "impossible" intermolecular multiple-quantum coherences (iMQCs) (*2–4*), specifically the zero-quantum coherences (iZQCs) (*2*) that correspond to simultaneously flipping two water spins in opposite directions on molecules separated by 10 μm to 1 mm (*3–8*). The iZQC linewidth (hence, the image contrast) is determined by local sus-

W. S. Warren and S. Ahn, Department of Chemistry, Princeton University, Princeton, NJ 08544–1009, USA. M. Mescher, M. Garwood, K. Ugurbil, Center for Magnetic Resonance Research, University of Minnesota, 385 East River Road, Minneapolis, MN 55455, USA. W. Richter, National Research Council Canada, Institute for Biodiagnostics, 435 Ellice Avenue, Winnipeg, MB R3B 1Y6, Canada. R. R. Rizi, J. Hopkins, J. S. Leigh, Department of Radiology, University of Pennsylvania, Philadelphia, PA 19104, USA.

*To whom correspondence should be addressed. E-mail: wwarren@princeton.edu